

# Truly Chiral Phonons Arising From Chirality-Selective Magnon-Phonon Coupling

Markus Weißenhofer,<sup>1,2,\*</sup> Philipp Rieger,<sup>1</sup> M. S. Mrudul,<sup>1</sup> Luca Mikadze,<sup>1</sup> Ulrich Nowak,<sup>3</sup> and Peter M. Oppeneer<sup>1</sup>

<sup>1</sup>*Department of Physics and Astronomy, Uppsala University, P. O. Box 516, S-751 20 Uppsala, Sweden*

<sup>2</sup>*Department of Physics, Freie Universität Berlin, Arnimallee 14, D-14195 Berlin, Germany*

<sup>3</sup>*Department of Physics, University of Konstanz, DE-78457 Konstanz, Germany*

(Dated: November 7, 2024)

Chiral phonons are desirable for applications in spintronics but their generation and control remains a challenge. Here we demonstrate the emergence of truly chiral phonons from selective magnon-phonon coupling in inversion-symmetric magnetic systems. Considering bcc Fe as example, we quantitatively calculate hybridized magnon-phonon quasiparticle states across the entire Brillouin zone utilizing first-principles calculations. Our findings challenge conventional magneto-elastic interpretations and reveal finite zero-point phonon angular momentum and strong anomalous Hall responses linked to finite (spin) Berry curvatures. Our results further establish that the existence of chiral phonons, particularly along high-symmetry directions, is common in many magnetic materials, offering promising avenues for novel spintronic and phononic devices.

*Introduction.* Chirality, which denotes the asymmetry between a structure and its mirror image, is one of the fundamental properties of matter [1]. In condensed matter physics, it plays a crucial role in the properties of fermionic and bosonic (quasi-)particles, such as electrons [2, 3], magnons [4–7], and phonons [8–11].

Recent theoretical predictions [8, 12] and experimental observations in two-dimensional materials [9] have identified phonon modes with finite angular momentum at high-symmetry points of the Brillouin zone (BZ), arising from the circular (or elliptical) orbital motions of atoms around their equilibrium lattice positions [10, 13]. Such phonon angular momentum plays a crucial role in a wide variety of effects ranging from the phonon Hall effect [14–17], the ultrafast Einstein-de Haas [18, 19] and Barnett effects [20, 21], magnon-phonon conversion [22], to phonon magnetic moments [10, 23–25].

While it has become common to refer to all phonons with finite angular momentum  $\mathbf{L}$  as chiral [8, 12], symmetry arguments suggest that non-propagating phonons and those propagating in the rotation plane do not possess true chiral character [26, 27]. To unambiguously define *truly* chiral phonons, we introduce the phonon chirality parameter  $\Sigma = \mathbf{L} \cdot \mathbf{v}/|\mathbf{v}|$ , where  $\mathbf{v}$  is the group velocity, based on the considerations presented in Ref. [27]. Truly chiral phonons are characterized by a finite  $\Sigma$  and have recently been experimentally detected in systems *lacking* inversion ( $\mathcal{P}$ ) symmetry [27, 28].

Here, we present fully quantitative, first-principles-based calculations to demonstrate the emergence of truly chiral phonons in the  $\mathcal{P}$ -symmetric ferromagnetic material bcc Fe as a result of phonon-chirality-selective magnon-phonon coupling. This coupling breaks time-reversal symmetry for the phonons and is derived from a recently developed framework describing the interaction between lattice and magnetic degrees of freedom [29, 30]. We further calculate a finite zero-point angular momentum [13] and intrinsic anomalous Hall responses of the coupled magnon-phonon quasiparticles.

*Phonon angular momentum.* As shown in Ref. [13], the angular momentum of the phononic system is given by

$$\mathbf{L} = \sum_{\mathbf{k}\lambda} \mathbf{L}_{\mathbf{k}\lambda} \left( n_{\mathbf{k}\lambda} + \frac{1}{2} \right), \quad \mathbf{L}_{\mathbf{k}\lambda} = 2\hbar \text{Re}[\boldsymbol{\chi}_{\mathbf{k}\lambda}] \times \text{Im}[\boldsymbol{\chi}_{\mathbf{k}\lambda}], \quad (1)$$

where  $n_{\mathbf{k}\lambda}$  is the phonon occupation number and the sum is over all phonon branches  $\lambda$  and wave vectors  $\mathbf{k}$  in the first BZ. In the absence of relativistic effects, the phonon frequencies  $\omega_{\mathbf{k}\lambda}$  and polarization vectors  $\boldsymbol{\chi}_{\mathbf{k}\lambda}$  are obtained from solving the eigenvalue problem  $\mathcal{D}_{\mathbf{k}} \boldsymbol{\chi}_{\mathbf{k}\lambda} = \omega_{\mathbf{k}\lambda}^2 \boldsymbol{\chi}_{\mathbf{k}\lambda}$  for the dynamical matrix  $\mathcal{D}_{\mathbf{k}}$  [13]. In inversion symmetric systems, to which we will restrict the discussion throughout the paper,  $\mathcal{D}_{\mathbf{k}}$  is real, and hence one can always choose  $\boldsymbol{\chi}_{\mathbf{k}\lambda} = e^{i\varphi_{\mathbf{k}\lambda}} \mathbf{e}_{\mathbf{k}\lambda}$ , with  $\mathbf{e}_{\mathbf{k}\lambda}$  being real and  $\varphi_{\mathbf{k}\lambda}$  an arbitrary phase. We call these phonon modes *linear*, as the associated dynamics of atoms are restricted to the one-dimensional space spanned by  $\mathbf{e}_{\mathbf{k}\lambda}$ . As such, the angular momentum  $\mathbf{L}_{\mathbf{k}\lambda}$  of all linear phonon modes trivially vanishes.

At a generic nonsymmetric point of the Brillouin zone, all phonon frequencies are different and the associated eigenvectors are unique (up to a phase). Consequently, all phonon modes at such points are linear and must have zero angular momentum, irrespective of representation. However, if two (or more) eigenvalues of the dynamical matrix coincide – e.g. at high-symmetry points, lines or planes – the eigenspace associated with this particular eigenvalue is two- (or higher-) dimensional. Considering e.g. two degenerate transverse phonon modes at some finite  $\mathbf{k}$  and  $\mathbf{v} \parallel \mathbf{k}$ , the corresponding eigenspace can be spanned by two real and orthonormal vectors  $\mathbf{e}_{\mathbf{k}1}$  and  $\mathbf{e}_{\mathbf{k}2}$ . They represent linear modes that can be superimposed to form left- and right-handed circular phonon modes,  $\boldsymbol{\chi}_{\mathbf{k}1} = (\mathbf{e}_{\mathbf{k}1} + i\mathbf{e}_{\mathbf{k}2})/\sqrt{2}$  and  $\boldsymbol{\chi}_{\mathbf{k}2} = (\mathbf{e}_{\mathbf{k}1} - i\mathbf{e}_{\mathbf{k}2})/\sqrt{2}$ . These modes correspond to the same eigenvalue as the linear modes, but they have a finite phonon chirality  $\Sigma = \pm\hbar$ , thus representing chiral phonon modes.

While high-symmetry regions with degenerate phonon

energies are certainly interesting from a fundamental perspective, they typically have little relevance for physical effects, as they occupy regions of the BZ with virtually no volume [31]. However, this changes when considering the impact of spin-lattice coupling (SLC) on the phonon band structure. This coupling can bridge the energy gap between two linear phonon modes, enabling them to couple and form a chiral phonon mode. Since SLC is generally a small correction to phonon energies [32], we expect chiral phonons in inversion-symmetric systems to only emerge in regions close to degenerate points, lines, and planes of the *bare* phonon spectrum [33]. This conjecture is demonstrated below, through fully quantitative calculations for the simple monoatomic ferromagnet bcc Fe, which serves here as example. The concepts can be readily applied to any other  $\mathcal{P}$ -symmetric magnetic system.

*Magnon-phonon coupling.* To describe the coupling of spin and lattice degrees of freedom (DoF) we adopt an atomistic approach. We start with the expansion of a phenomenological spin-lattice Hamiltonian up to the third order in DoF,

$$\begin{aligned} \hat{\mathcal{H}}_{\text{SLC}} = & \sum_i \frac{\hat{P}_i^2}{2m} + \sum_{ij,\alpha\beta} \left( \Phi_{ij}^{\alpha\beta} \hat{X}_i^\alpha \hat{X}_j^\beta + J_{ij}^{\alpha\beta} \hat{S}_i^\alpha \hat{S}_j^\beta \right) \\ & + \sum_{ijk,\alpha\beta\gamma} \left( J_{ijk}^{\alpha\beta\gamma} \hat{S}_i^\alpha \hat{S}_j^\beta \hat{X}_k^\gamma + G_{ijk}^{\alpha\beta\gamma} \hat{S}_i^\alpha \hat{X}_j^\beta \hat{P}_k^\gamma \right), \end{aligned} \quad (2)$$

keeping all terms compatible with inversion and (global) time-reversal symmetry. Here,  $\hat{S}_i^\alpha$  are vector spin operators at the site  $i$  with amplitude  $|\hat{S}_i^\alpha| = S$  and  $\hat{X}_i^\alpha$  and  $\hat{P}_i^\alpha$  are nuclear displacement and momentum operators. The first three terms of  $\hat{\mathcal{H}}_{\text{SLC}}$  are the kinetic energy of the atoms (of mass  $m$ ), the lattice potential (with the force constants  $\Phi_{ij}^{\alpha\beta}$  being the Fourier transform of the dynamical matrix  $\mathcal{D}_{\mathbf{k}}^{\alpha\beta}$ ) and the generalized Heisenberg interaction [34], where the  $J_{ij}^{\alpha\beta}$  also includes magneto-crystalline anisotropy (MCA). The antisymmetric Dzyaloshinskii–Moriya interaction (DMI) is forbidden by inversion symmetry.

Coupling between spin and lattice DoF arises from the last two terms of  $\hat{\mathcal{H}}_{\text{SLC}}$ . The term quadratic in spins and linear in displacements was recently introduced by Hellsvik *et al.* [29], and since then efficient methods to calculate all  $J_{ijk}^{\alpha\beta\gamma}$  parameters from first-principles have been established [30, 35–37].

The last term has gained little attention in the general form expressed here. Particularly, efficient methods to calculate the full set of  $G_{ijk}^{\alpha\beta\gamma}$  parameters from first principles are yet to be established. Instead, studies so far mainly investigated two special cases of this term: (i) a purely local term  $\sim \sum_i \hat{S}_i \cdot (\hat{X}_i \times \hat{P}_i)$  was used in a semi-classical description of atomic motion in the effective field of the spin [10, 20, 38], and (ii) a term obtained by fixing the spin orientation,  $\sum_{jk,\beta\gamma} G_{ijk}^{\beta\gamma} \hat{X}_j^\beta \hat{P}_k^\gamma$ , that appears e.g. in the Born-Huang approximation [31, 32, 39–41].

Magnon and phonon variables can be introduced via the Holstein-Primakoff transformation [42] and normal mode expansion (details in SM [43]). For a ferromagnetic state along  $z$ , the magnon-phonon Hamiltonian up to second order in magnon ( $\hat{b}_{\mathbf{k}}^{(\dagger)}$ ) and phonon operators ( $\hat{a}_{\mathbf{k},\lambda}^{(\dagger)}$ ) reads  $\hat{\mathcal{H}}_{\text{mp}} = \sum_{\mathbf{k}} \hat{\mathcal{H}}_{\mathbf{k}}$  with

$$\begin{aligned} \hat{\mathcal{H}}_{\mathbf{k}} = & \sum_{\lambda} \hbar\omega_{\mathbf{k}\lambda} \hat{a}_{\mathbf{k}\lambda}^{\dagger} \hat{a}_{\mathbf{k}\lambda} + \varepsilon_{\mathbf{k}} \hat{b}_{\mathbf{k}}^{\dagger} \hat{b}_{\mathbf{k}} \\ & + \sum_{\lambda} (c_{\mathbf{k}\lambda}^{-} \hat{b}_{-\mathbf{k}} + c_{\mathbf{k}\lambda}^{+} \hat{b}_{\mathbf{k}}^{\dagger}) (\hat{a}_{\mathbf{k}\lambda} + \hat{a}_{-\mathbf{k}}^{\dagger}) \\ & + \sum_{\lambda\lambda'} g_{\mathbf{k}\lambda\lambda'} (\hat{a}_{\mathbf{k}\lambda} + \hat{a}_{-\mathbf{k}\lambda}^{\dagger}) (\hat{a}_{-\mathbf{k}\lambda'} - \hat{a}_{\mathbf{k}\lambda'}^{\dagger}). \end{aligned} \quad (3)$$

Here,  $\varepsilon_{\mathbf{k}}$  are the bare magnon energies and zero point energies have been dropped. The magnon-phonon couplings  $c_{\mathbf{k}\lambda}^{\pm} = \sum_{\gamma} \sqrt{\hbar S^3 / m \omega_{\mathbf{k}\lambda}} (\tilde{J}_{\mathbf{k}}^{x z \gamma} \pm i \tilde{J}_{\mathbf{k}}^{y z \gamma}) \chi_{\mathbf{k}\lambda}^{\gamma}$  and phonon-phonon couplings  $g_{\mathbf{k}\lambda\lambda'} = -\frac{i}{2} \hbar S \sqrt{\omega_{\mathbf{k}\lambda'} / \omega_{\mathbf{k}\lambda}} \sum_{\beta\gamma} \tilde{G}_{\mathbf{k}}^{z\beta\gamma} \chi_{\mathbf{k}\lambda}^{\beta} (\chi_{\mathbf{k}\lambda'}^{\gamma})^*$  depend on the Fourier transforms  $\tilde{J}_{\mathbf{k}}^{\alpha\beta\gamma} = \sum_{jk} e^{i\mathbf{k}\cdot(\mathbf{r}_k - \mathbf{r}_j)} J_{ijk}^{\alpha\beta\gamma}$  and  $\tilde{G}_{\mathbf{k}}^{\alpha\beta\gamma} = \sum_{jk} e^{i\mathbf{k}\cdot(\mathbf{r}_j - \mathbf{r}_k)} G_{ijk}^{\alpha\beta\gamma}$  of the coefficients of the third order terms in Eq. (2). They are relativistic corrections to the bare modes and proportional to spin-orbit coupling [30, 32]. The emergence of chiral phonons has been previously linked to the phonon-phonon coupling term proportional to  $g_{\mathbf{k}\lambda\lambda'}$  [13, 31, 41]. Hereinafter we will omit the phonon-phonon coupling  $g_{\mathbf{k}\lambda\lambda'}$  and instead focus on the magnon-phonon coupling  $c_{\mathbf{k}\lambda}^{\pm}$ . We show that magnon-phonon coupling can give rise to truly chiral phonons in bcc Fe.

For this purpose we use  $J_{ijk}^{\alpha\beta\gamma}$  coefficients that were recently calculated from first-principles [30]. The bare magnon energies follow  $\varepsilon_{\mathbf{k}} = S(2d + 2 \sum_j J_{ij} [1 - e^{-i\mathbf{k}\cdot(\mathbf{r}_j - \mathbf{r}_i)}])$ , where the isotropic exchange constants  $J_{ij} = \frac{1}{3} \sum_{\alpha} J_{ij}^{\alpha\alpha}$  are also taken from first-principles calculations [44] and the MCA energy  $d$  is from experiments [45]. The bare phonon frequencies and polarization vectors are calculated using the density-functional perturbation theory implementation of Quantum ESPRESSO [46, 47]. Both the bare magnon and phonon bandstructures are shown in the SM [43].

*Coupled magnon-phonon bandstructure.* The exact diagonalization of Eq. (3) is performed numerically using Colpa’s method [48]. The energies of the four bands along different high-symmetry paths in the BZ are shown in Fig. 1, focusing on the regions with greatest modification of the energies compared to the bare modes. The longitudinal acoustic (LA) phonon does not couple to magnons and is thus unaltered by SLC.

We observe *avoided crossings* where the bare modes intersect, which indicate the formation of hybrid magnon-phonon quasiparticles, the so-called *magnon polarons* [49]. The energy gaps between the hybridizing modes range from around 0.18 meV to

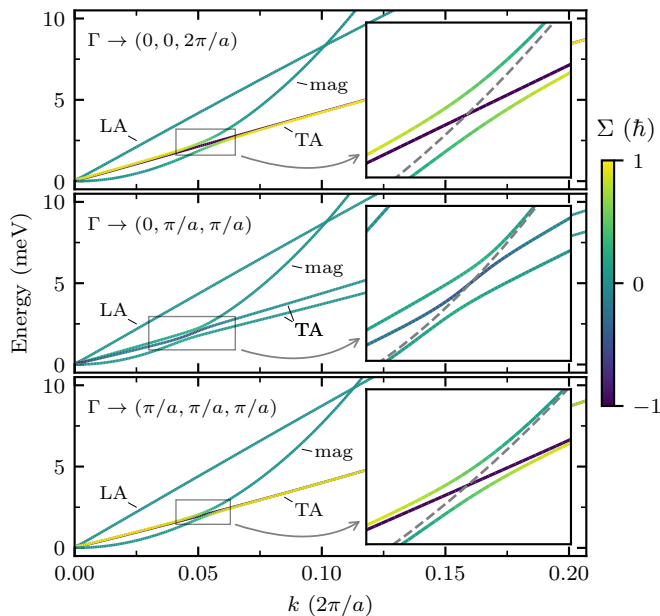


Figure 1. Coupled magnon-phonon bands in bcc Fe calculated along various high-symmetry paths of the BZ starting from  $\Gamma = (0, 0, 0)$ . Labels LA, TA, and mag indicate the predominant character of the mode far away from the avoided crossings and the colors encode the phonon chirality  $\Sigma = \mathbf{L} \cdot \mathbf{v}/|\mathbf{v}|$ , with  $\mathbf{v} = \partial\omega/\partial\mathbf{k}$  being the group velocity. The insets zoom in on the avoided crossings (indicated by the small grey rectangles), and the grey dashed lines are the bare magnon energies. Note that the bare TA modes are degenerate for  $\Gamma \rightarrow (0, 0, 2\pi/a)$  and  $\Gamma \rightarrow (\pi/a, \pi/a, \pi/a)$ .

0.45 meV. Physically, the magnon-phonon coupling contains an antisymmetric, DMI-like contribution,  $c_{\mathbf{k}\lambda}^{\pm,a} = \frac{1}{2} \sum_{\gamma} \sqrt{\hbar S^3/m\omega_{\mathbf{k}\lambda}} [(\tilde{J}_{\mathbf{k}}^{xz\gamma} - \tilde{J}_{\mathbf{k}}^{zx\gamma}) \pm i(\tilde{J}_{\mathbf{k}}^{yz\gamma} - \tilde{J}_{\mathbf{k}}^{zy\gamma})] \chi_{\mathbf{k}\lambda}^{\gamma}$  and a symmetric, two-site anisotropy-like contribution  $c_{\mathbf{k}\lambda}^{\pm,s} = \frac{1}{2} \sum_{\gamma} \sqrt{\hbar S^3/m\omega_{\mathbf{k}\lambda}} [(\tilde{J}_{\mathbf{k}}^{xz\gamma} + \tilde{J}_{\mathbf{k}}^{zx\gamma}) \pm i(\tilde{J}_{\mathbf{k}}^{yz\gamma} + \tilde{J}_{\mathbf{k}}^{zy\gamma})] \chi_{\mathbf{k}\lambda}^{\gamma}$ , both of which are of relativistic origin. In bcc Fe, the DMI-like coupling greatly exceeds the symmetric one [30]. Therefore, the widely-used conventional magneto-elastic theory [50] is unable to describe the magnon-phonon dispersion calculated here, as it lacks a term related to DMI. Such a term was only recently derived [51] from the atomistic SLC Hamiltonian (2). In the light of this so-far overlooked DMI-like coupling, established interpretations of magnon-phonon hybridization based on conventional magneto-elastic theory [52–56] has to be reconsidered.

As one key result of this paper, we find that the magnon mode only hybridizes with one of the TA modes, if the two bare TA phonons are degenerate. In the non-degenerate case, i.e.,  $\Gamma$  to  $(0, \pi/a, \pi/a)$ , there are two avoided crossings with both TA modes in close proximity. Calculating the phonon chirality  $\Sigma$  for these magnon-phonon modes, we reveal that the magnons selectively couple to phonons with one chirality. We note that upon reversal of the magnetization from  $z$  to  $-z$ , the magnons

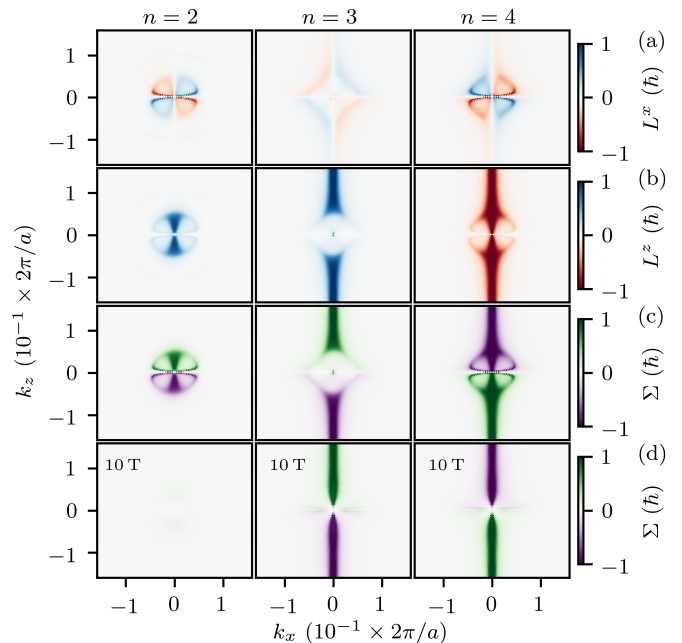


Figure 2. Phonon angular momenta and chiralities of the coupled magnon-phonon bands computed for bcc Fe. Plots in each row illustrate (a)  $L^x$ , (b)  $L^z$ , (c)  $\Sigma$  without applied magnetic field, and (d)  $\Sigma$  with a field of  $B = 10$  T for the different magnon-phonon modes with label  $n \in \{2, 3, 4\}$ . The mode with  $n = 1$  (LA phonon) is achiral and hence not shown.  $L^y$  is zero in the  $k_x$ - $k_z$  plane depicted here.

instead only couple to phonons with opposite chirality. We further emphasize that the magnon-phonon coupling also lifts the degeneracy of the phonons far away from the avoided crossing regions, leading to a small energy gap of the order of 1  $\mu\text{eV}$  between the two chiral phonon modes. Selective hybridization between magnons and non-propagating circularly polarized phonons has been measured recently in the layered zigzag antiferromagnet FePSe<sub>3</sub> [57].

The phonon angular momentum and chirality in the  $k_x$ - $k_z$  plane of the BZ are shown in Fig. 2 (results for other planes are discussed in the SM [43]). As argued above, truly chiral phonons primarily occur in close proximity of the high symmetry axes – here, the  $k_z$  axis – where they arise as a superposition of the degenerate bare TA phonons. Note that phonons along  $k_x$  and  $k_y$  remain linear. This symmetry breaking arises from the orientation of magnetization along the  $z$ -direction in combination with spin-orbit coupling [58].

The emergence of chiral phonons in a roughly circular pattern around the  $\Gamma$  point [see Fig. 2(a),(b)] is a result of magnon-phonon hybridization. This can be demonstrated by applying an external magnetic field in the direction of the magnetization. A magnetic field  $B$  shifts the bare magnon energies by  $\varepsilon_{\mathbf{k}} \rightarrow \varepsilon_{\mathbf{k}} + \mu_s B$ , with  $\mu_s = 2.2 \mu_B$  being the saturation magnetic moment of bcc Fe [59]. For field strengths of  $B = 10$  T the energies of

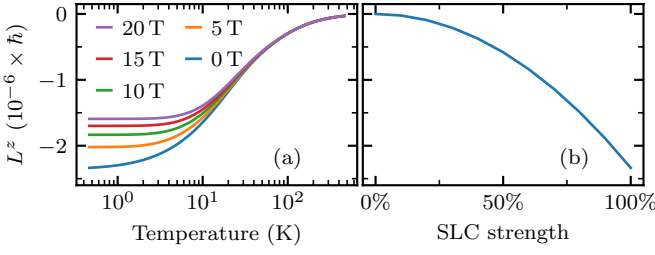


Figure 3. Nonzero component  $L_z$  of the equilibrium phonon angular momentum per unit cell for bcc Fe, shown in (a) versus temperature and for applied magnetic fields as labeled and in (b) versus rescaled SLC strength.

the bare magnons are way above those of the TA phonons [60], making avoided crossings impossible and confining the chiral phonons to the vicinity of the  $k_z$ -direction, see Fig. 2(d). This proves that magnon-phonon coupling can induce chiral phonons without direct hybridization with magnons, i.e., if their energies are very different.

Next, we calculate the equilibrium phonon angular momentum for bcc Fe via Eq (1), see Fig. 3. In thermal equilibrium the occupation numbers of a magnon-phonon state with energy  $\varepsilon_{\mathbf{k}n}$  follow the Bose-Einstein distribution,  $n_{\mathbf{k}n} = 1/(e^{\varepsilon_{\mathbf{k}n}/k_B T} - 1)$ . The scaling of the equilibrium phonon angular momentum with temperature  $T$  is shown in Fig. 3(a). Surprisingly, we find that the system has a small, but finite *zero-point angular momentum*  $\mathbf{L}(T \rightarrow 0) = \sum_{\mathbf{k}n} \frac{1}{2} \mathbf{L}_{\mathbf{k}n}$  [13], because the angular momenta of the different modes do not fully cancel. Moreover, it is observed that the equilibrium phonon angular momentum vanishes in the limit of high temperatures. By changing the applied magnetic field we can eliminate the impact of BZ regions with avoided crossings on  $\mathbf{L}$ , revealing the dominant role of chiral phonons without substantial hybridization with magnons in the high-temperature limit. To further elucidate the concept of zero-point angular momentum, we vary the strength of SLC from 0% to 100% [Fig. 3(b)]. This scaling highlights that the angular momentum arises solely from relativistic effects, emphasizing the intrinsic link between spin-orbit coupling and the observed zero-point contributions.

*Intrinsic anomalous Hall responses.* Nontrivial (spin) Berry curvature arising due to magnon-polaron formation can lead to the emergence of Hall-type quantum transport phenomena of heat and spin angular momentum, manifested in thermal Hall and spin Nernst effects [61–63]. The Berry curvature of the  $n$ th band can be obtained by casting the Hamiltonian in a Bogoliubov-de Gennes form [64], which gives

$$\Omega_{\mu\nu}^n(\mathbf{k}) = 2i\hbar^2 \sum_{m \neq n}^{2N_b} g_{nm} g_{mm} \frac{\langle n_{\mathbf{k}} | \hat{v}_\mu | m_{\mathbf{k}} \rangle \langle m_{\mathbf{k}} | \hat{v}_\nu | n_{\mathbf{k}} \rangle}{[(g\mathcal{E}_{\mathbf{k}})_{nn} - (g\mathcal{E}_{\mathbf{k}})_{mm}]^2}, \quad (4)$$

where  $|n_{\mathbf{k}}\rangle$  is an eigenstate of  $\hat{\mathcal{H}}_{\mathbf{k}}$ ,  $N_b$  is the num-

ber of magnon-phonon bands,  $\mathcal{E}_{\mathbf{k}} = \text{diag}(\varepsilon_{\mathbf{k}1}, \dots, \varepsilon_{\mathbf{k}N_b}, \varepsilon_{-\mathbf{k}1}, \dots, \varepsilon_{-\mathbf{k}N_b})$  is a matrix containing the eigenenergies,  $\hat{\mathbf{v}} = \hbar^{-1} \partial_{\mathbf{k}} \hat{\mathcal{H}}_{\mathbf{k}}$  is the velocity operator and  $g = \sigma_z \otimes \mathbb{1}_{N_d \times N_d}$ , with  $\sigma_z$  being the  $z$  component of the Pauli matrices and  $\mathbb{1}_{N_b \times N_b}$  the unit matrix of dimension  $N_b$ . For details, we refer to Ref. [62].

Hereinafter, we consider an ultrathin, quasi-two dimensional layer of bcc Fe by restricting the  $\mathbf{k}$  values to a plane through the BZ that includes  $\Gamma$ . Integrating the Berry curvature of the  $n$ th band over such plane yields the respective first Chern number  $C_n$ . E.g., for the  $k_x$ - $k_y$  plane it reads  $C_n = \frac{1}{2\pi} \int dk_x dk_y \Omega_{xy}^n(\mathbf{k})$ . Even though we obtain finite Berry curvatures as a result of time-reversal symmetry breaking via the SLC, Chern numbers of the magnon-phonon bands are zero, i.e., the bandstructure is topologically trivial [65]. This is because there are two topological gaps, one at the aforementioned avoided crossing region and a second one close to  $\Gamma$ , with an opposite sign of Berry curvature. Note that for calculating the Chern numbers, we apply a small magnetic field of  $B \geq 0.5$  T to broaden the Berry curvature close to  $\Gamma$ .

The anomalous magnon-phonon thermal Hall conductivity  $\kappa_{\mu\nu}$  and the spin Nernst coefficient  $\alpha_{\mu\nu}^{S\tau}$ , respectively, relate a transverse heat current and a transverse spin current to an applied temperature gradient, expressed as  $J_\mu = -\sum_\nu \kappa_{\mu\nu} \partial_\nu T$  and  $J_\mu^{S\tau} = -\sum_\nu \alpha_{\mu\nu}^{S\tau} \partial_\nu T$ . Within linear response theory,  $\kappa_{\mu\nu}$  is related to the Berry curvature via [66–69]

$$\kappa_{\mu\nu} = -\frac{k_B^2 T}{\hbar \mathcal{A}} \sum_{\mathbf{k}} \sum_{n=1}^{N_b} c_2(n_{\mathbf{k}n}) \Omega_{\mu\nu}^n(\mathbf{k}), \quad (5)$$

where  $\mathcal{A}$  is the area of the system and  $c_2(x) = (1+x) \ln \frac{1+x}{x} - (\ln x)^2 - 2\text{Li}_2(-x)$ , with  $\text{Li}_2(x)$  being the second order polylogarithm function. Similarly, the spin Nernst coefficient  $\alpha_{\mu\nu}^{S\tau}$  can be obtained from the spin Berry curvature  $\Omega_{\mu\nu}^{S\tau, n}(\mathbf{k})$  via [61, 70, 71]

$$\alpha_{\mu\nu}^{S\tau} = -\frac{2k_B}{\mathcal{A}} \sum_{\mathbf{k}} \sum_{n=1}^{N_b} c_1(f(\varepsilon_{\mathbf{k}n})) \Omega_{\mu\nu}^{S\tau, n}(\mathbf{k}), \quad (6)$$

$$\Omega_{\mu\nu}^{S\tau, n}(\mathbf{k}) = 2i\hbar^2 \sum_{m \neq n}^{2N_b} g_{nm} g_{mm} \frac{\langle n_{\mathbf{k}} | \hat{j}_\mu^{S\tau} | m_{\mathbf{k}} \rangle \langle m_{\mathbf{k}} | \hat{v}_\nu | n_{\mathbf{k}} \rangle}{[(g\mathcal{E}_{\mathbf{k}})_{nn} - (g\mathcal{E}_{\mathbf{k}})_{mm}]^2}, \quad (7)$$

with  $c_1(x) = (1+x) \ln(1+x) - x \ln x$ , and  $\hat{j}_\mu^{S\tau} = \frac{1}{4} \{\hat{v}_\mu, g\hat{S}_\tau\}$ .

Both anomalous transport coefficients, calculated for an ultrathin Fe(001) film by summing  $\mathbf{k}$  over the  $k_x$ - $k_y$  plane, are shown in Fig. 4. They turn out to be significantly larger than what has been calculated previously for magnon-polaron bands in honeycomb ferro- [62] and ferrimagnets [61]. This is because in bcc Fe the magnon-phonon modes with finite (spin) Berry curvature have rather low energies, thus contributing strongly to transport. By varying the applied magnetic field, we further

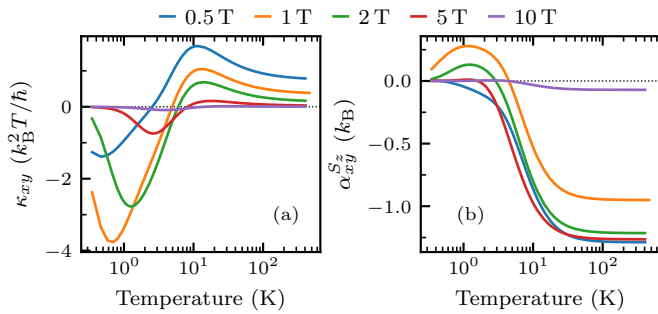


Figure 4. Anomalous thermal Hall conductivity (a) and spin Nernst coefficient (b) due to magnon-polarons in an ultrathin Fe(001) film. The magnetization is in out-of-plane direction and a magnetic field with values as labeled is applied in the same direction.

demonstrate the tunability of  $\kappa_{xy}$  and  $\alpha_{xy}^{S_z}$ . As mentioned earlier, strong applied fields suppress the hybridization of magnons and phonons by shifting the bare magnon energies above those of the transverse acoustic TA phonons. This underscores that the emergence of intrinsic anomalous Hall responses is fundamentally linked to the formation of magnon-polaron hybrid bands.

*Conclusions.* We have demonstrated the existence of truly chiral phonons arising from chirality-selective magnon-phonon coupling in inversion-symmetric magnetic systems. Our first-principles-based approach provides a robust, quantitative framework for understanding the hybridized magnon-phonon quasiparticle states across the entire BZ. Given that magnon-phonon coupling in bcc Fe is primarily influenced by a DMI-like term, we conclude that previous interpretations of magnon-phonon hybridization based on conventional magneto-elastic theory, which does not account for such a term, must be reconsidered. We further reveal the existence of a finite zero-point phonon angular momentum – an entirely quantum mechanical phenomenon without classical counterpart – emerging from the intricate coupling between phononic zero-point fluctuations and those of the spin angular momenta. Additionally, we observe strong and tunable anomalous Hall responses arising from finite (spin) Berry curvatures associated with magnon-phonon hybridization.

Our results imply that the existence of truly chiral phonons along high-symmetry directions, featuring at least two degenerate bare phonon modes, is an abundant characteristic in many magnetic materials. Since the ability to control and utilize these chiral phonons opens new avenues for transporting angular momentum and manipulating magnetic order, this finding will certainly prove useful in the search for potential material candidates for novel spintronic or phononic devices.

M.W. and P.M.O. acknowledge support from the German Research Foundation (Deutsche Forschungsgemeinschaft) through CRC/TRR 227 “Ultrafast Spin Dynam-

ics” (Project MF, Project ID No. 328545488). U.N. acknowledges support from the Germany Research Foundation through CRC 1432. This work has furthermore been supported by the Swedish Research Council (VR), the Knut and Alice Wallenberg Foundation (Grants No. 2022.0079 and No. 2023.0336), and by the EIC Pathfinder OPEN grant No. 101129641 (OBELIX). The calculations were enabled by resources provided by the National Academic Infrastructure for Supercomputing in Sweden (NAISS) at NSC Linköping partially funded by the Swedish Research Council through grant agreement No. 2022-06725.

\* markus.weissenhofer@fu-berlin.de

- [1] R. S. Cahn, Christopher Ingold, and V. Prelog, “Specification of Molecular Chirality,” *Angew. Chem. Intern. Ed.* **5**, 385–415 (1966).
- [2] Su-Yang Xu, Ilya Belopolski, Nasser Alidoust, Madhab Neupane, Guang Bian, Chenglong Zhang, Raman Sankar, Guoqing Chang, Zhujun Yuan, Chi-Cheng Lee, Shin-Ming Huang, Hao Zheng, Jie Ma, Daniel S. Sanchez, BaoKai Wang, Arun Bansil, Fangcheng Chou, Pavel P. Shibayev, Hsin Lin, Shuang Jia, and M. Zahid Hasan, “Discovery of a Weyl fermion semimetal and topological Fermi arcs,” *Science* **349**, 613–617 (2015).
- [3] Guoqing Chang, Benjamin J. Wieder, Frank Schindler, Daniel S. Sanchez, Ilya Belopolski, Shin-Ming Huang, Bahadur Singh, Di Wu, Tay-Rong Chang, Titus Neupert, Su-Yang Xu, Hsin Lin, and M. Zahid Hasan, “Topological quantum properties of chiral crystals,” *Nature Mater.* **17**, 978–985 (2018).
- [4] B. Roessli, P. Böni, W. E. Fischer, and Y. Endoh, “Chiral Fluctuations in MnSi above the Curie Temperature,” *Phys. Rev. Lett.* **88**, 237204 (2002).
- [5] Y. Nambu, J. Barker, Y. Okino, T. Kikkawa, Y. Shiomi, M. Enderle, T. Weber, B. Winn, M. Graves-Brook, J. M. Tranquada, T. Ziman, M. Fujita, G. E. W. Bauer, E. Saitoh, and K. Kakurai, “Observation of Magnon Polarization,” *Phys. Rev. Lett.* **125**, 027201 (2020).
- [6] Yahui Liu, Zhengmeng Xu, Lin Liu, Kai Zhang, Yang Meng, Yuanwei Sun, Peng Gao, Hong-Wu Zhao, Qian Niu, and J. Li, “Switching magnon chirality in artificial ferrimagnet,” *Nature Commun.* **13**, 1264 (2022).
- [7] Libor Šmejkal, Alberto Marmodoro, Kyo-Hoon Ahn, Rafael González-Hernández, Ilja Turek, Sergiy Mankovsky, Hubert Ebert, Sunil W. D’Souza, O. Šipr, Jairo Sinova, and T. Jungwirth, “Chiral Magnons in Altermagnetic RuO<sub>2</sub>,” *Phys. Rev. Lett.* **131**, 256703 (2023).
- [8] Lifa Zhang and Qian Niu, “Chiral Phonons at High-Symmetry Points in Monolayer Hexagonal Lattices,” *Phys. Rev. Lett.* **115**, 115502 (2015).
- [9] Hanyu Zhu, Jun Yi, Ming-Yang Li, Jun Xiao, Lifa Zhang, Chih-Wen Yang, Robert A. Kaindl, Lain-Jong Li, Yuan Wang, and Xiang Zhang, “Observation of chiral phonons,” *Science* **359**, 579–582 (2018).
- [10] Dominik M. Juraschek and Nicola A. Spaldin, “Orbital magnetic moments of phonons,” *Phys. Rev. Mater.* **3**, 064405 (2019).

- [11] Tingting Wang, Hong Sun, Xiaozhe Li, and Lifa Zhang, “Chiral Phonons: Prediction, Verification, and Application,” *Nano Lett.* **24**, 4311–4318 (2024).
- [12] Hao Chen, Wei Zhang, Qian Niu, and Lifa Zhang, “Chiral phonons in two-dimensional materials,” *2D Materials* **6**, 012002 (2018).
- [13] Lifa Zhang and Qian Niu, “Angular Momentum of Phonons and the Einstein–de Haas Effect,” *Phys. Rev. Lett.* **112**, 085503 (2014).
- [14] C. Strohm, G. L. J. A. Rikken, and P. Wyder, “Phenomenological Evidence for the Phonon Hall Effect,” *Phys. Rev. Lett.* **95**, 155901 (2005).
- [15] G. Grissonnanche, S. Thériault, A. Gourgout, M.-E. Boulanger, E. Lefrançois, A. Ataei, F. Laliberté, M. Dion, J.-S. Zhou, S. Pyon, T. Takayama, H. Takagi, N. Doiron-Leyraud, and L. Taillefer, “Chiral phonons in the pseudogap phase of cuprates,” *Nature Phys.* **16**, 1108–1111 (2020).
- [16] Sungjoon Park and Bohm-Jung Yang, “Phonon Angular Momentum Hall Effect,” *Nano Lett.* **20**, 7694–7699 (2020).
- [17] B. Flebus and A. H. MacDonald, “Phonon Hall Viscosity of Ionic Crystals,” *Phys. Rev. Lett.* **131**, 236301 (2023).
- [18] C. Dornes, Y. Acremann, M. Savoini, M. Kubli, M. J. Neugebauer, E. Abreu, L. Huber, G. Lantz, C. A. F. Vaz, H. Lemke, E. M. Bothschafter, M. Porer, V. Esposito, L. Rettig, M. Buzzi, A. Alberca, Y. W. Windsor, P. Beaud, U. Staub, Diling Zhu, Sanghoon Song, J. M. Glowia, and S. L. Johnson, “The ultrafast Einstein–de Haas effect,” *Nature* **565**, 209–212 (2019).
- [19] S. R. Tauchert, M. Volkov, D. Ehberger, D. Kazenwadel, M. Evers, H. Lange, A. Donges, A. Book, W. Kreuzpaintner, U. Nowak, and P. Baum, “Polarized phonons carry angular momentum in ultrafast demagnetization,” *Nature* **602**, 73–77 (2022).
- [20] Jiaming Luo, Tong Lin, Junjie Zhang, Xiaotong Chen, Elizabeth R. Blackert, Rui Xu, Boris I. Yakobson, and Hanyu Zhu, “Large effective magnetic fields from chiral phonons in rare-earth halides,” *Science* **382**, 698–702 (2023).
- [21] C. S. Davies, F. G. N. Fennema, A. Tsukamoto, I. Razdolski, A. V. Kimel, and A. Kirilyuk, “Phononic switching of magnetization by the ultrafast Barnett effect,” *Nature* **628**, 540–544 (2024).
- [22] J. Holanda, D. S. Maior, A. Azevedo, and S. M. Rezende, “Detecting the phonon spin in magnon–phonon conversion experiments,” *Nature Phys.* **14**, 500–506 (2018).
- [23] Dominik M. Juraschek, Michael Fechner, Alexander V. Balatsky, and Nicola A. Spaldin, “Dynamical multiferroicity,” *Phys. Rev. Mater.* **1**, 014401 (2017).
- [24] Yafei Ren, Cong Xiao, Daniyar Saparov, and Qian Niu, “Phonon Magnetic Moment from Electronic Topological Magnetization,” *Phys. Rev. Lett.* **127**, 186403 (2021).
- [25] M. Basini, M. Pancaldi, B. Wehinger, M. Udina, V. Unikandanunni, T. Tadano, M. C. Hoffmann, A. V. Balatsky, and S. Bonetti, “Terahertz electric-field-driven dynamical multiferroicity in SrTiO<sub>3</sub>,” *Nature* **628**, 534–539 (2024).
- [26] Sang-Wook Cheong and Xianghan Xu, “Magnetic chirality,” *npj Quantum Mater.* **7**, 40 (2022).
- [27] Hiroki Ueda, Mirian García-Fernández, Stefano Agrestini, Carl P. Romao, Jeroen van den Brink, Nicola A. Spaldin, Ke-Jin Zhou, and Urs Staub, “Chiral phonons in quartz probed by X-rays,” *Nature* **618**, 946–950 (2023).
- [28] Kyosuke Ishito, Huiling Mao, Yusuke Kousaka, Yoshihiko Togawa, Satoshi Iwasaki, Tiantian Zhang, Shuichi Murakami, Jun-ichiro Kishine, and Takuya Satoh, “Truly chiral phonons in  $\alpha$ -HgS,” *Nature Phys.* **19**, 35–39 (2023).
- [29] Johan Hellsvik, Danny Thonig, Klas Modin, Diana Iuşan, Anders Bergman, Olle Eriksson, Lars Bergqvist, and Anna Delin, “General method for atomistic spin-lattice dynamics with first-principles accuracy,” *Phys. Rev. B* **99**, 104302 (2019).
- [30] Sergiy Mankovsky, Svitlana Polesya, Hannah Lange, Markus Weißenhofer, Ulrich Nowak, and Hubert Ebert, “Angular Momentum Transfer via Relativistic Spin-Lattice Coupling from First Principles,” *Phys. Rev. Lett.* **129**, 067202 (2022).
- [31] Sinisa Coh, “Classification of materials with phonon angular momentum and microscopic origin of angular momentum,” *Phys. Rev. B* **108**, 134307 (2023).
- [32] Shang Ren, John Bonini, Massimiliano Stengel, Cyrus E. Dreyer, and David Vanderbilt, “Adiabatic Dynamics of Coupled Spins and Phonons in Magnetic Insulators,” *Phys. Rev. X* **14**, 011041 (2024).
- [33] (), We use the term *bare* modes to describe phonon or magnon modes in the absence of spin-lattice coupling.
- [34] Ulrich Nowak, “Classical spin models,” in *Handbook of Magnetism and Advanced Magnetic Materials*, edited by H Kronmüller and S Parkin (John Wiley & Sons, Ltd, 2007).
- [35] Hannah Lange, Sergiy Mankovsky, Svitlana Polesya, Markus Weißenhofer, Ulrich Nowak, and Hubert Ebert, “Calculating spin-lattice interactions in ferro- and antiferromagnets: The role of symmetry, dimension, and frustration,” *Phys. Rev. B* **107**, 115176 (2023).
- [36] Sergiy Mankovsky, Hannah Lange, Svitlana Polesya, and Hubert Ebert, “Spin-lattice interaction parameters from first principles: Theory and implementation,” *Phys. Rev. B* **107**, 144428 (2023).
- [37] I. P. Miranda, M. Pankratova, M. Weißenhofer, A. B. Klautau, D. Thonig, M. Pereiro, E. Sjöqvist, A. Delin, M. I. Katsnelson, O. Eriksson, and A. Bergman, “Spin-lattice couplings in 3d ferromagnets: analysis from first-principles,” (2024), arXiv:2409.18274 [cond-mat.mtrl-sci].
- [38] Tom Kahana, Daniel A. Bustamante Lopez, and Dominik M. Juraschek, “Light-induced magnetization from magnonic rectification,” *Sci. Adv.* **10**, eado0722 (2024).
- [39] C. Alden Mead and Donald G. Truhlar, “On the determination of Born–Oppenheimer nuclear motion wave functions including complications due to conical intersections and identical nuclei,” *J. Chem. Phys.* **70**, 2284–2296 (1979).
- [40] Max Born and Kun Huang, *Dynamical Theory Of Crystal Lattices* (Oxford University Press, 1996).
- [41] Lifa Zhang, Jie Ren, Jian-Sheng Wang, and Baowen Li, “The phonon Hall effect: theory and application,” *J. Phys.: Condens. Matter* **23**, 305402 (2011).
- [42] T. Holstein and H. Primakoff, “Field Dependence of the Intrinsic Domain Magnetization of a Ferromagnet,” *Phys. Rev.* **58**, 1098–1113 (1940).
- [43] See Supplemental Material for the derivation of magnon-phonon Hamiltonian, the bare bandstructures, and the results for phonon angular momentum and chirality in other planes of the BZ.

- [44] O. N. Mryasov, A. J. Freeman, and A. I. Liechtenstein, “Theory of non-Heisenberg exchange: Results for localized and itinerant magnets,” *J. Appl. Phys.* **79**, 4805–4807 (1996).
- [45] Ilya Razdolski, Alexandr Alekhin, Nikita Ilin, Jan P. Meyburg, Vladimir Roddatis, Detlef Diesing, Uwe Bovensiepen, and Alexey Melnikov, “Nanoscale interface confinement of ultrafast spin transfer torque driving non-uniform spin dynamics,” *Nature Commun.* **8**, 15007 (2017).
- [46] Paolo Giannozzi, Stefano Baroni, Nicola Bonini, Matteo Calandra, Roberto Car, Carlo Cavazzoni, Davide Ceresoli, Guido L Chiarotti, Matteo Cococcioni, Ismaila Dabo, Andrea Dal Corso, Stefano de Gironcoli, Stefano Fabris, Guido Fratesi, Ralph Gebauer, Uwe Gerstmann, Christos Gougousis, Anton Kokalj, Michele Lazzeri, Layla Martin-Samos, Nicola Marzari, Francesco Mauri, Riccardo Mazzarello, Stefano Paolini, Alfredo Pasquarello, Lorenzo Paulatto, Carlo Sbraccia, Sandro Scandolo, Gabriele Scaluzero, Ari P Seitsonen, Alexander Smogunov, Paolo Umari, and Renata M Wentzcovitch, “QUANTUM ESPRESSO: a modular and open-source software project for quantum simulations of materials,” *J. Phys.: Condens. Matter* **21**, 395502 (2009).
- [47] P Giannozzi, O Andreussi, T Brumme, O Bunau, M Buongiorno Nardelli, M Calandra, R Car, C Cavazzoni, D Ceresoli, M Cococcioni, N Colonna, I Carnimeo, A Dal Corso, S de Gironcoli, P Delugas, R A DiStasio, A Ferretti, A Floris, G Fratesi, G Fugallo, R Gebauer, U Gerstmann, F Giustino, T Gorni, J Jia, M Kawamura, H-Y Ko, A Kokalj, E Küçükbenli, M Lazzeri, M Marsili, N Marzari, F Mauri, N L Nguyen, H-V Nguyen, A Otero de-la Roza, L Paulatto, S Poncé, D Rocca, R Sabatini, B Santra, M Schlipf, A P Seitsonen, A Smogunov, I Timrov, T Thonhauser, P Umari, N Vast, X Wu, and S Baroni, “Advanced capabilities for materials modelling with Quantum ESPRESSO,” *J. Phys.: Condens. Matter* **29**, 465901 (2017).
- [48] J.H.P. Colpa, “Diagonalization of the quadratic boson hamiltonian,” *Physica A: Statistical Mechanics and its Applications* **93**, 327–353 (1978).
- [49] Yi Li, Chenbo Zhao, Wei Zhang, Axel Hoffmann, and Valentyn Novosad, “Advances in coherent coupling between magnons and acoustic phonons,” *APL Materials* **9**, 060902 (2021).
- [50] Charles Kittel, “Physical Theory of Ferromagnetic Domains,” *Rev. Mod. Phys.* **21**, 541–583 (1949).
- [51] Markus Weisshofer, Hannah Lange, Akashdeep Kamra, Sergiy Mankovsky, Svitlana Polesya, Hubert Ebert, and Ulrich Nowak, “Rotationally invariant formulation of spin-lattice coupling in multiscale modeling,” *Phys. Rev. B* **108**, L060404 (2023).
- [52] R. M. White, M. Sparks, and I. Ortenburger, “Diagonalization of the Antiferromagnetic Magnon-Phonon Interaction,” *Phys. Rev.* **139**, A450–A454 (1965).
- [53] Andreas Rückriegel, Peter Kopietz, Dmytro A. Bozhko, Alexander A. Serga, and Burkard Hillebrands, “Magnetoelastic modes and lifetime of magnons in thin yttrium iron garnet films,” *Phys. Rev. B* **89**, 184413 (2014).
- [54] Akashdeep Kamra, Hedyeh Keshtgar, Peng Yan, and Gerrit E. W. Bauer, “Coherent elastic excitation of spin waves,” *Phys. Rev. B* **91**, 104409 (2015).
- [55] Simon Streib, Nicolas Vidal-Silva, Ka Shen, and Gerrit E. W. Bauer, “Magnon-phonon interactions in magnetic insulators,” *Phys. Rev. B* **99**, 184442 (2019).
- [56] Alexander G Gurevich and Gennadii A Melkov, *Magnetization oscillations and waves* (CRC press, 2020).
- [57] Jun Cui, Emil Viñas Boström, Mykhaylo Ozerov, Fanguang Wu, Qianni Jiang, Jiun-Haw Chu, Changcun Li, Fucui Liu, Xiaodong Xu, Angel Rubio, and Qi Zhang, “Chirality selective magnon-phonon hybridization and magnon-induced chiral phonons in a layered zigzag antiferromagnet,” *Nature Commun.* **14**, 3396 (2023).
- [58] Mildred S Dresselhaus, Gene Dresselhaus, and Ado Jorio, *Group theory: application to the physics of condensed matter* (Springer Science & Business Media, 2007).
- [59] R F L Evans, W J Fan, P Chureemart, T A Ostler, M O A Ellis, and R W Chantrell, “Atomistic spin model simulations of magnetic nanomaterials,” *J. Phys.: Condens. Matter* **26**, 103202 (2014).
- [60] (), A minimum of  $B \approx 4.5$  T is needed to shift the bare magnons energies above those of the bare TA phonons.
- [61] Sungjoon Park, Naoto Nagaosa, and Bohm-Jung Yang, “Thermal Hall Effect, Spin Nernst Effect, and Spin Density Induced by a Thermal Gradient in Collinear Ferromagnets from Magnon-Phonon Interaction,” *Nano Lett.* **20**, 2741–2746 (2020).
- [62] Jostein N. Kløgetvedt and Alireza Qaiumzadeh, “Tunable topological magnon-polaron states and intrinsic anomalous Hall phenomena in two-dimensional ferromagnetic insulators,” *Phys. Rev. B* **108**, 224424 (2023).
- [63] Song Bao, Zhao-Long Gu, Yanyan Shangguan, Zhentao Huang, Junbo Liao, Xiaoxue Zhao, Bo Zhang, Zhao-Yang Dong, Wei Wang, Ryoichi Kajimoto, Mitsutaka Nakamura, Tom Fennell, Shun-Li Yu, Jian-Xin Li, and Jinsheng Wen, “Direct observation of topological magnon polarons in a multiferroic material,” *Nature Commun.* **14**, 6093 (2023).
- [64] Alexander Mook, Jürgen Henk, and Ingrid Mertig, “Thermal Hall effect in noncollinear coplanar insulating antiferromagnets,” *Phys. Rev. B* **99**, 014427 (2019).
- [65] Cui-Zu Chang, Chao-Xing Liu, and Allan H. MacDonald, “Colloquium: Quantum anomalous hall effect,” *Rev. Mod. Phys.* **95**, 011002 (2023).
- [66] Lifa Zhang, “Berry curvature and various thermal Hall effects,” *New J. Phys.* **18**, 103039 (2016).
- [67] Ryo Matsumoto, Ryuichi Shindou, and Shuichi Murakami, “Thermal Hall effect of magnons in magnets with dipolar interaction,” *Phys. Rev. B* **89**, 054420 (2014).
- [68] Shuichi Murakami and Akihiro Okamoto, “Thermal hall effect of magnons,” *J. Phys. Soc. Jpn.* **86**, 011010 (2017).
- [69] Xiao-Tian Zhang, Yong Hao Gao, and Gang Chen, “Thermal Hall effects in quantum magnets,” *Phys. Rep.* **1070**, 1–59 (2024).
- [70] Gyungchoon Go and Se Kwon Kim, “Tunable large spin Nernst effect in a two-dimensional magnetic bilayer,” *Phys. Rev. B* **106**, 125103 (2022).
- [71] Bo Li, Shane Sandhoefer, and Alexey A. Kovalev, “Intrinsic spin Nernst effect of magnons in a noncollinear antiferromagnet,” *Phys. Rev. Res.* **2**, 013079 (2020).